Miniaturized fiber inline Fabry–Perot interferometer fabricated with a femtosecond laser

Tao Wei,[1] Yukun Han,[2] Hai-Lung Tsai,[2] and Hai Xiao[1,*]

[1]*Department of Electrical and Computer Engineering, Missouri University of Science and Technology, 1870 Miner Circle, Rolla, Missouri 65409-0040, USA*

[2]*Department of Mechanical and Aerospace Engineering, Missouri University of Science and Technology, 1870 Miner Circle, Rolla, Missouri 65409-0040, USA*

**Corresponding author: xiaoha@mst.edu*

Received November 6, 2007; revised January 25, 2008; accepted February 1, 2008; posted February 11, 2008 (Doc. ID 89498); published March 5, 2008

We report a miniaturized inline Fabry–Perot interferometer directly fabricated on a single-mode optical fiber with a femtosecond laser. The device had a loss of 16 dB and an interference visibility exceeding 14 dB. The device was tested and survived in high temperatures up to 1100°C. With an accessible cavity and all-glass structure, the new device is attractive for sensing applications in high-temperature harsh environments. © 2008 Optical Society of America

OCIS codes: 050.2230, 060.2370, 120.3180.

Optical fiber Fabry–Perot (FP) interferometric sensors have been well demonstrated for various sensing applications in the past. The FP cavity can be either intrinsic (e.g., a section of fiber between two dielectric mirrors [1]) or extrinsic (e.g., an air gap between two cleaved fiber endfaces [2]). The two reflections at the two end surfaces of the FP cavity form an interference signal that is a function of the length and refractive index of the cavity. The deflection of the cavity due to changes in environment causes a phase shift in the interference pattern. As a result, a fiber FP sensor is capable of measuring various parameters including temperature, pressure, strain, acoustics, and flow. With advantages such as small size, immunity to electromagnetic interference (EMI), and corrosion resistance, these fiber FP sensors are particularly attractive for applications involving harsh environments [3,4].

Various methods have been reported to fabricate fiber extrinsic FP sensors in the past, evolving from epoxy-based assembly in the early days [5] to the more recent fusion-based assembly using a CO_2 laser [3] or an electric arc fusion splicer [6]. These methods involve complicated procedures of assembling multiple components together. The length of the cavity varies in each device, and the performance is neither predictable nor controllable. The multiple parts assembly also compromises the robustness of the device owing to the limited strength of the joints. The mismatch of the coefficient of thermal expansion (CTE) of the various parts can also seriously lower the thermal stability of the device. As a result, the demonstrated devices have shown limited capability to survive high temperatures.

The latest advancement in femtosecond laser technology has opened a new window of opportunity for one-step fabrication of microdevices with true three-dimensional (3D) configurations. Direct exposure of most solid materials (including fused silica glass) to ultraintense femtosecond laser pulses results in the quick establishment of free electron plasma at the focal point, leading to the ablation of a thin layer of materials [7]. Femtosecond laser pulses with extremely high peak power produce almost no thermal damage as the pulse duration is shorter than the thermalization time [8]. Due to the muliphoton nature of the interaction, the ablation process can be conducted on the material surface as well as within its bulk. Femtosecond lasers have been successfully used for directly writing optical waveguides [9,10] and micromachining microchannels and microchambers in glasses [11].

In this Letter, we report a novel fiber inline FP interferometer (FPI) structure with an open cavity formed by one-step micromachining a micronotch in a single-mode optical fiber using a femtosecond laser. The device has an all-glass structure and does not involve the assembly of multiple components. As a result, we expect that the device will survive very high temperatures. In addition, the accessible FP cavity makes it possible to be used as an ultracompact chemical sensor based on refractive index measurement.

The device fabrication was carried out using a home-integrated femtosecond laser 3D micromachining system as schematically shown in Fig. 1. The repetition rate, center wavelength, and pulse width of the femtosecond laser (Legend-F, Coherent, Inc.) were 1 kHz, 800 nm, and 120 fs, respectively. The maximum output power of the femtosecond laser was

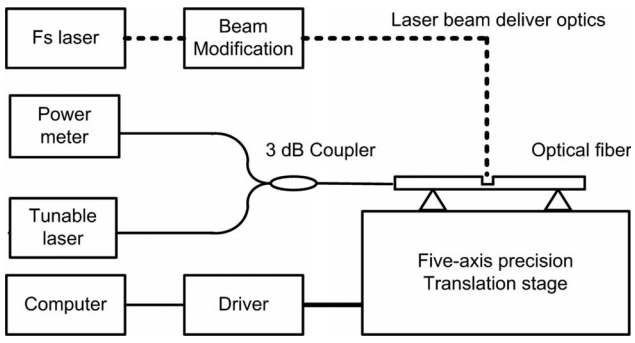

Fig. 1. Fiber inline FPI device fabrication system using a femtosecond laser.

~1 W. We used the combination of wave plates and polarizers to reduce the laser power to about 20 mW and then used several neutral density (ND) filters to further reduce the laser power to desirable values. The attenuated laser beam was directed into an objective lens (Olympus UMPLFL 20X) with a numerical aperture (NA) of 0.45 and focused onto the single-mode optical fiber (Corning SMF 28) mounted on a computer-controlled five-axis translation stage (Aerotech, Inc.) with a resolution of 1 μm.

During fabrication, the interference signal of the fiber FP device was continuously monitored. A tunable laser source (HP 8168E) was connected to one of the input ports of the 3 dB fiber coupler. The output port of the coupler was connected to the device under fabrication. Controlled by the computer, the tunable laser continuously scanned through its wavelength range (1475–1575 nm) at the rate of 1 nm per step. The signal reflected from the device at each wavelength step was recorded by an optical power meter (Agilent 8163A). The fabrication was stopped after a well-formed interference pattern was recorded.

Figure 2 shows the schematic structure and scanning electron microscope (SEM) images of the fabricated fiber FP device. Figure 2(b) shows that a micronotch was formed on the optical fiber. Figure 2(c) shows the femtosecond laser ablated surface. The cavity length was about 30 μm as estimated from the SEM image. The depth of ablation was ~72 μm, just passing the fiber core. The FP cavity can be made very close (within a few hundreds of micrometers) to the end of the fiber. With such a short bending arm, the chance of bending-induced device breakage is small.

Figure 3 shows the interference spectrum of an in-line fiber FPI device fabricated by the femtosecond laser. The background loss of this particular device was about 16 dB. This relatively high loss was mainly caused by three reasons: (1) the light scattering loss at the laser-ablated surface; (2) the nonperpendicular surface orientation with respect to the fiber axis, which was partially evidenced by the nonflat interference peak intensities shown in Fig. 2;

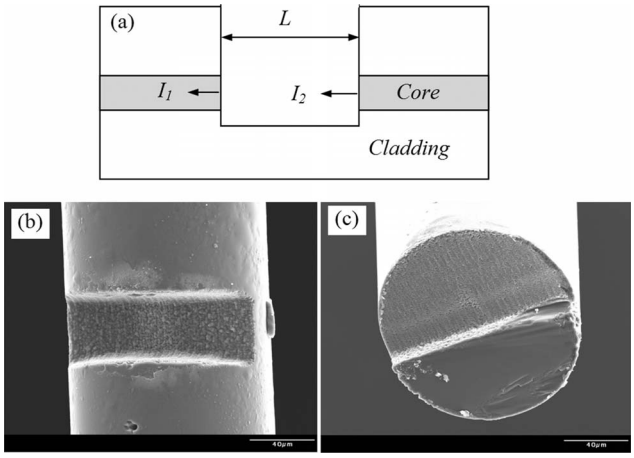

Fig. 2. Schematic structure and SEM images of fiber in-line FPI device fabricated by femtosecond laser ablation. (a) Structural illustration, (b) top view, and (c) cross section.

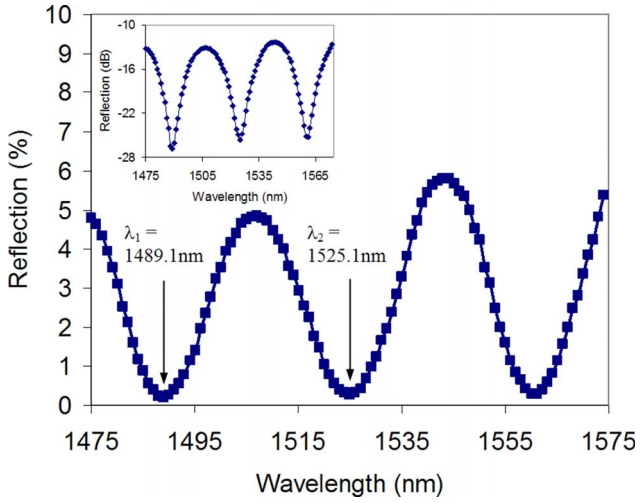

Fig. 3. (Color online) Interference spectrum of the fabricated fiber inline FPI device. Inset, interference fringe plotted in dB scale.

and (3) the coupling loss as a result of recoupling the light reflected from the second endface of the FP cavity back into the fiber core. We believe that the surface roughness can be reduced by reducing the laser scanning steps, of course, at the expense of a long device fabrication time. The nonperpendicular surface orientation can also be minimized by careful adjustment of the stages. The coupling loss increases with the length of the FP cavity. As a result, it may eventually limit the practical length of the cavity. Nevertheless, the interference spectrum indicated a high fringe visibility, exceeding 14 dB, which is sufficient for most sensing applications.

Due to the low reflectivity of the laser-ablated surface, multiple reflections have negligible contributions to the optical interference. The low-finesse FP device can thus be modeled using the two-beam optical interference equation [12,13]

$$I = I_1 + I_2 + 2\sqrt{I_1 I_2}\cos\left(\frac{4\pi L}{\lambda} + \varphi_0\right), \tag{1}$$

where I is the intensity of the interference signal; I_1 and I_2 are the reflections at the cavity surfaces, respectively; φ_0 is the initial phase of the interference; L is the optical length of the cavity; and λ is the optical wavelength.

According to Eq. (1), the two adjacent interference minimums have a phase difference of 2π. That is,

$$\left(\frac{4\pi L}{\lambda_1} + \varphi_0\right) - \left(\frac{4\pi L}{\lambda_2} + \varphi_0\right) = 2\pi, \tag{2}$$

where λ_1 and λ_2 are the wavelengths of two adjacent valleys (Fig. 3) in the interference spectrum. The optical length of the FP cavity can thus be found as $L = 0.5\lambda_1\lambda_2/(\lambda_2 - \lambda_1)$. Based on the interference spectrum shown in Fig. 3, we calculated that the FP cavity length was 30.797 μm, which was very close to the length estimated by SEM imaging.

The fabricated device was tested for its ability to survive high temperatures. The sensor was placed

horizontally in a quartz tube with a 1 in. (25.4 nm) inner diameter, hosted inside a programmable electric tubular furnace. The temperature of the furnace was increased from room temperature to 1100°C (limited by the highest temperature of the furnace used) at a step of 50°C, and the interference spectra at these temperatures were recorded using a similar interrogation system as shown in Fig. 1. However, to improve the accuracy, we replaced the tunable laser with a broadband source made by multiplexing C-band and L-band erbium-doped fiber amplified spontaneous emission (ASE) sources. The interference fringe reflected from the device was recorded by an optical spectrum analyzer (OSA, HP 70952B).

The cavity length as a function of the temperature is plotted in Fig. 4, where it increased nearly linearly following the increase of temperature. The fiber FP device successfully survived high temperatures up to 1100°C. However, as temperature increased to 1100°C, the interference fringe visibility was dropped by about 2 dB compared to that at room temperature. The temperature sensitivity of this particular FP device was estimated to be 0.074 pm/°C based on the linear fit of the measurement data. The equivalent CTE of the device was calculated to be 2.4×10^{-6}/°C, which was about four times larger than the known CTE of the fiber cladding (fused silica, 5.5×10^{-7}/°C). The thermal test was repeated several times and the results were quite reproducible. Repositioning of the fiber and the device did not produce observable changes in the cavity length within the accuracy of the measurement and at any testing temperature, indicating that the pigtail bending effect was not a major contribution to the large equivalent CTE. Therefore, we concluded that the large device CTE was mainly caused by the thermally induced bending of the asymmetric FP structure, partially evidenced by the decreasing interference visibility at high temperatures. More experiments are currently underway to study the causes of such thermal behavior, which will be a subject of future publication.

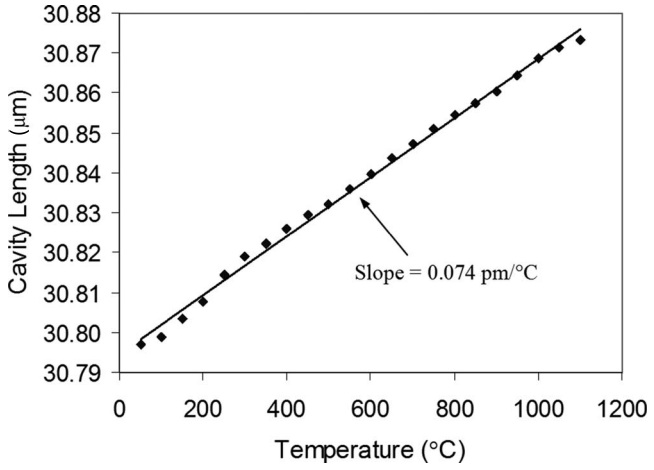

Fig. 4. Fiber inline FP device in response to temperature change.

To summarize, a novel fiber inline FP device with an accessible cavity was fabricated by one-step femtosecond laser micromaching. Although the roughness of the laser-ablated surfaces introduced a considerable background loss, the fringe visibility of the device was high enough for most sensing applications. The device successfully survived high temperatures up to 1100°C. The device may be directly utilized for temperature sensing or strain monitoring in harsh environments. However, more detailed characterizations and/or calibrations are necessary before such a device can be used as a sensor. More importantly, the unique accessible FP cavity makes it attractive to develop ultracompact chemical sensors based on refractive index measurement.

The research work was supported by the Office of Naval Research through the Young Investigator Program (N00014-07-0008) and the American Chemical Society through the Petroleum Research Fund (PRF-43927).

References

1. C. E. Lee and H. F. Taylor, Electron. Lett. **24**, 193 (1988).
2. R. O. Claus, M. F. Gunther, A. Wang, and K. A. Murphy, J. Smart Mater. Struct. **1**, 237 (1992).
3. A. Wang, H. Xiao, J. Wang, Z. Wang, W. Zhao, and R. G. May, J. Lightwave Technol. **19**, 1495 (2001).
4. H. Xiao, J. Deng, G. Pickrell, R. G. May, and A. Wang, J. Lightwave Technol. **21**, 2276 (2003).
5. V. Bhatia, K. A. Murphy, R. O. Claus, M. E. Jones, J. L. Grace, T. A. Tran, and J. A. Greene, Meas. Sci. Technol. **7**, 58 (1996).
6. Y. Zhang, X. Chen, Y. Wang, K. L. Cooper, and A. Wang, J. Lightwave Technol. **25**, 1797 (2007).
7. M. Li, S. Menon, J. P. Nibarger, and G. N. Gibson, Phys. Rev. Lett. **82**, 2394 (1999).
8. L. Jiang and H. L. Tsai, J. Appl. Phys. **100**, 023116 (2005).
9. K. M. Davis, K. Miura, N. Sugimoto, and K. Hirao, Opt. Lett. **21**, 1729 (1996).
10. A. Szameit, D. Bloemer, J. Burghoff, T. Pertsch, S. Nolte, F. Lederer, and A. Tuennermann, Appl. Phys. B **82**, 507 (2006).
11. H. Sun, F. He, Z. Zhou, Y. Cheng, Z. Xu, K. Sugioka, and K. Midorikawa, Opt. Lett. **32**, 1536 (2007).
12. E. Hecht, *Optics*, 4th ed. (Addison Wesley, 2002).
13. B. Qi, G. R. Pickrell, J. Xu, P. Zhang, Y. Duan, W. Peng, Z. Huang, W. Huo, H. Xiao, R. G. May, and A. Wang, Opt. Eng. **42**, 3165 (2003).